

# Pedestrian Motion Classification for Autonomous Vehicles (6.867 Final Project)

Michael Everett & Björn Lütjens

**Abstract**—In this project, we applied techniques from the course to a dataset of pedestrian trajectories recorded on a golf cart around MIT’s campus. Our main objective was to classify whether a pedestrian’s trajectory would enter a 4x10m rectangle in front of the vehicle, which could be used as an active safety feature on various types of vehicles that interact with pedestrians. We trained a SVM with Gaussian RBF Kernel and optimized hyperparameters to achieve 86.3% test accuracy. We then trained an RNN for the same task and achieved 80.4% test accuracy. Finally, we experimented with pedestrian motion prediction, to predict the future pedestrian trajectory, which is more complicated than binary classification.

## I. INTRODUCTION

Autonomous vehicles use onboard sensors to perceive their surroundings, and use the data to make decisions about where it is safe to drive. Today’s research vehicles typically rely on Lidar and cameras as the main sensors, as these provide information about where/what obstacles are, and can help the vehicle maintain safe position in its lane and with respect to obstacles. In addition to static obstacles, vehicles interact with pedestrians in a variety of environments: people in crosswalks, jaywalkers, kids running across neighborhood streets. A campus shuttle could even drive on sidewalks among pedestrians, so the vehicle would be interacting with pedestrians almost all the time. These regular interactions mean the vehicle must be able to predict pedestrians’ next moves in order to maintain safety.

Pedestrian motion prediction is difficult because people often behave very unexpectedly. Humans use many strategies to predict pedestrian intent while driving, such as body language, eye contact, and other non-verbal cues between human driver and human pedestrian, but autonomous vehicles can’t easily communicate or read these signals. The information from sensors is typically fused: Lidar is used to measure the pedestrian position, and the camera is used to label the particular obstacle as a pedestrian. Therefore the only measurements collected are position over time (from which velocity can also be computed).

This project uses a dataset collected on MIT’s campus over several months by three golf cart shuttles providing Mobility on Demand service to students, while simultaneously collecting pedestrian trajectory data to optimize vehicle routing strategy. The dataset contains about 65,000 pedestrian trajectories as well as the vehicles’ trajectories, all in a global frame across the MIT campus.

We omit a thorough literature review section for the sake of brevity – relevant works that are specifically used in the project are cited throughout.



(a) Ground robot in Stata



(b) Golf carts (MIT MoD fleet)

Fig. 1: Many types of autonomous vehicles operate among pedestrians and must account for pedestrian motion in the vehicle motion planning algorithms.

The objective of this project is to develop a classifier that can determine whether a person will step in front of a vehicle, based on a few seconds of their trajectory. We use a portion of our data set to train different classifiers, optimize hyperparameters with a separate portion, and evaluate performance with yet another portion. This classifier could be a useful component of an autonomous vehicle, or part of an active safety feature on a human-driven vehicle that could take over in case the driver does not see a pedestrian in time.

The main contributions of this work are (i) an SVM classifier for predicting when pedestrians will step in front of a vehicle, (ii) a classifier using LSTMs for that same objective, and (iii) initial results for pedestrian motion prediction using LSTMs.

## II. DATASET

An important realization we made during this project is the challenge of working with a real dataset. Understanding the raw data became a significant portion of the project, so this chapter provides a thorough explanation of our findings and methods to process the data.

### A. Raw Data

Our data comes from golf carts equipped with Lidar and cameras [1], [2]. Fortunately, it is relatively straightforward to visualize trajectory data, as opposed to some high-dimensional datasets that exist for other applications.

The raw dataset’s fields are shown in Table I, where (easting,northing) are the latitude/longitude global coordinates, and (x,y) are the coordinates in our global campus map. Veh id indicates which of the three vehicles corresponds to that data point, or in the pedestrian case, which vehicle sensed that pedestrian. Ped id is a unique id given to each pedestrian seen.

There are some noise-related issues with the raw data, as it was collected on a research vehicle under development.

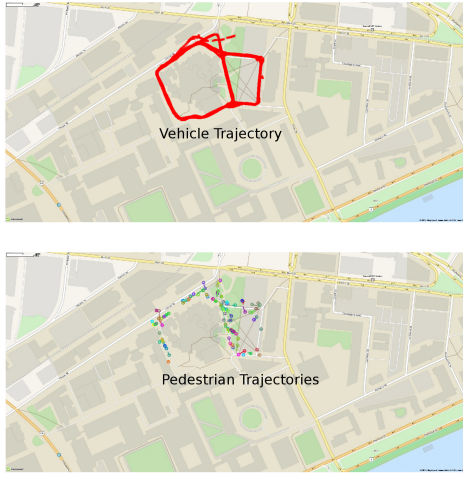


Fig. 2: The raw trajectories from one day of data collection visualized on a campus map. All trajectories are recorded in the global map coordinate frame.

| Type       | Fields |         |          |   |   |        |        |
|------------|--------|---------|----------|---|---|--------|--------|
| Vehicle    | time   | easting | northing | x | y | veh id |        |
| Pedestrian | time   | easting | northing | x | y | veh id | ped id |

TABLE I: Raw data fields

One issue is that the vehicle’s (x,y) position sometimes jumps, because the vehicle’s localization system does not use GPS and is imperfect. Other minor issues include pedestrian trajectories that incorrectly split/merge or are too short to be useful for this project.

In addition to addressing noise, we also pre-process the data by converting pedestrian trajectories into the vehicle’s local frame. Our objective is to classify whether pedestrians cross in front of the vehicle, so the pedestrian trajectories must be converted into the vehicle’s local frame. That is, our dataset is initially unlabeled, and we must generate the ground truth label that we wish to learn to classify later.

It might be possible to somehow feed both the vehicle trajectory and pedestrian trajectory into a classifier, and have it learn the transformation, but it seemed much more straightforward for us to rotate the data ahead of time. Using global coordinates could potentially allow the classifier to learn a global understanding of the map (e.g. where sidewalks/intersections are), but we chose to focus on a more structured problem for this project. Since global coordinates should have an impact on pedestrian motion, we could in the future try a hybrid approach where we feed local coordinates along with some context features (e.g. distance to curb, traffic light state) as in [3].

### B. Global-to-Local Transformation

The global-to-local transformation relies on knowledge of vehicle orientation (heading angle) and smooth vehicle trajectories, neither of which we have by default. The global-to-local transformation projects the vehicle-to-pedestrian relative position vector onto the coordinate frame that points straight out of the vehicle’s front and left side. Line 1 describes the

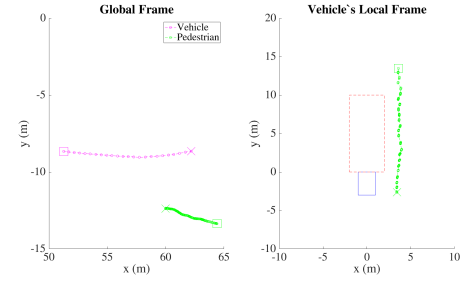


Fig. 3: On the left, the vehicle trajectory (magenta) and pedestrian trajectory (green) in the global frame. Both start from the square and move to the X. On the right is the local vehicle frame: the vehicle is the blue rectangle, and the red dashed rectangle is the “cross” zone. The green pedestrian trajectory doesn’t cross into the red rectangle, so this trajectory is given binary label 0.

procedure for filtering, transforming, and labeling the raw dataset.

The transformation is visualized in Fig. 3. On the left, the global frame shows the vehicle (magenta) moving from left to right, and the pedestrian moving from bottom right toward the left. Therefore, the pedestrian is moving along the vehicle’s right side. This is exactly what we see in the vehicle’s local frame on the right plot.

---

#### Algorithm 1: Algorithm for extracting local trajectories

---

**Input:**  $V_g, P_g$ : global vehicle, pedestrian trajectories (Table I)

**Output:**  $P_l$ : pedestrian trajectories in local vehicle frame

- 1: **for** each vehicle **do**
  - 2:  $I_{posjump} = \{i \in [1, \text{len}(V_g) - 1] \mid \text{euclid.dist}(V_g(i) - V_g(i+1)) > 1.0\}$
  - 3:  $I_{timejump} = \{i \in [1, \text{len}(V_g) - 1] \mid \text{time}(V_g(i) - V_g(i+1)) > 0.5\}$
  - 4:  $J = I_{posjump} \cup I_{timejump}$
  - 5:  $T_{valid} = \{[J(i), J(i+1)] \mid \text{time}(J(i+1) - J(i)) > 5.0\}$   
M. E. finish
  - 6: **return** pedestrian trajectories
- 

### C. Processed Dataset

The processed dataset is visualized in Fig. 4. The vehicle (yellow taxi) has a blue rectangle representing the “cross” zone (similar to Fig. 3). Green trajectories are local pedestrian trajectories that do not cross into the blue zone, and red trajectories are ones that do enter the blue zone.

A few important observations about the processed dataset are the jaggedness and locations of trajectories. The jaggedness is due to the transformation and sensor rates: the Lidar provides pedestrian trajectory at high rate (50 Hz), but the vehicle position is updated at a slower rate (10 Hz), so the pedestrian trajectory jumps a bit each time vehicle time step. Since the rotation is dependent on vehicle heading angle, and vehicle heading angle is computed from consecutive vehicle

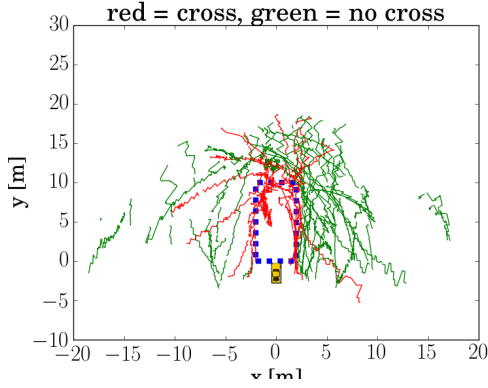


Fig. 4: A small portion of the training set for the binary classifier. The vehicle (yellow taxi) has a blue rectangle representing the “cross” zone. Green trajectories are local pedestrian trajectories that do not cross into the blue zone, and red ones do.

positions, this process is subject to some noise. It is also somewhat difficult to imagine what local trajectories *should* look like, because these trajectories are showing how the vehicle and pedestrian move relative to one another, and an observer doesn’t know what the vehicle’s velocity was for any particular trajectory. For example, a trajectory that arcs along the front of the vehicle could be the vehicle turning as a pedestrian walks straight, or a pedestrian walking in a curve while the vehicle is parked. All of this could have been avoided if we had access to raw sensor measurements, as these provide local coordinates by default.

The second observation is that the trajectories are in front/along the sides of the vehicle, and have a limited range of about 20m. This makes sense given our sensor: it is mounted on the vehicle’s front and sees a 270° cone. Its maximum range is more than 20m, but tracking pedestrians reliably is difficult beyond this distance.

### III. SVM BINARY CLASSIFIER

We trained a Support Vector Machine (SVM) to do binary classification on local pedestrian trajectories, to predict whether the trajectory will/will not enter a 4x10m rectangle in front of the vehicle. A portion of the pedestrian trajectory is fed into the classifier, and it outputs a binary label. This could be a useful safety feature on a car to identify which pedestrians might cross in front of the vehicle.

The trajectories are all of different length, so we split them up into equal “snippets” of length  $l$ . Each trajectory has a single 0/1 label, and this same label is applied to each snippet. This allows us to learn some notion of direction from (x,y) sequences, because a snippet that never crosses in front of the vehicle can still be labeled as such, if a later portion of its trajectory eventually does cross in front. These  $l$ -long lists of (x,y) points are fed into the classifier as the feature vector of length  $2l$ , as:  $(x_i = [x_1, y_1, x_2, y_2, \dots, x_l, y_l]; y_i = 0/1)$ .

We used the SKLearn implementation of SVM [4] with Gaussian RBF Kernel.

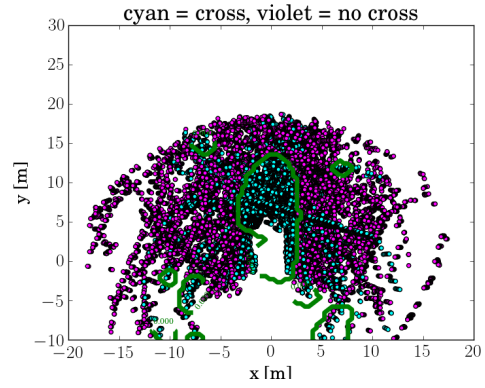


Fig. 5: SVM trained on snippets with  $l = 1$  allow visualization of decision boundary. The important part of this plot is the green decision boundary in the center that resembles our arbitrary “cross zone”. The SVM has roughly learned the location/shape of zone for simple input data. There is some overfitting evident by other green regions, but this is likely more of an artifact of  $l = 1$  hyperparameter.

#### A. Simple Example

We first tried training with  $l = 1$ , so that we could easily visualize the decision boundary in Fig. 5. The data (magenta/cyan) aren’t particularly meaningful, because it’s hard to learn anything from a single (x,y) position of a pedestrian ( $l = 1$ ). But, we can observe that the green decision boundary roughly resembles our arbitrarily-created rectangular “cross zone”. This figure indicates the SVM is correctly learning that there is a region in space that causes trajectories to be labeled a certain way. After this quick sanity check, we can proceed to larger values of  $l$ , but lose the ability to easily visualize the results.

#### B. Hyperparameters

There are several hyperparameters that affect the behavior of the classifier. The main ones that we experimented with were  $l$  (snippet length) and  $C$  (SVM regularizer). A grid search for optimal parameter values is shown in Table II (optimal w.r.t. high validation accuracy). Because of the time required to train so many combinations (especially affected by Gaussian RBF Kernel), we trained on a smaller subset of the training set during hyperparameter optimization.

As  $C$  increases, training accuracy increases for all scenarios, which is expected because this corresponds to more penalty on mis-classified points. We can tell when  $C$  is too high, because training accuracy is much higher than validation accuracy, a symptom of overfitting.

As  $l$  increases, more time steps of pedestrian positions are used in the feature vector, so there is more information on which to classify. Intuitively, large  $l$  would seem preferable than small, but if  $l$  is too large, the noise in the data may outweigh the value of the information. To be more concrete, it seems unlikely that one would need 50 points worth of trajectory data to do the binary classification (especially given the noise seen in Fig. 4).

This intuition aligns with our observed validation accuracies. The highest validation accuracy of 79.8% occurs with

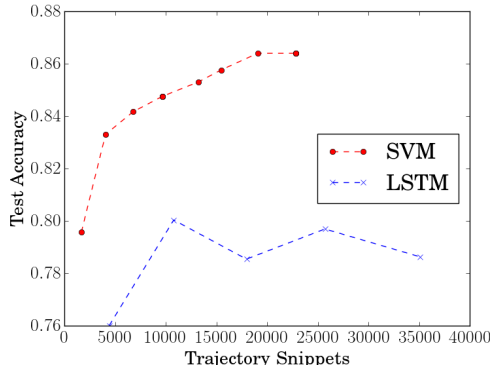


Fig. 6: Effect of training set size on SVM and LSTM binary classifiers. As expected, test accuracy increases with more training data, but levels off after about 20k trajectory snippets for SVM, and 10k for LSTM.

$l = 25$  and  $C = 10$ , so we choose those as the optimal hyperparameters.

The test accuracy with these values was 74.4%.

### C. Training Set Size

Another parameter that affects classifier accuracy is size of training set. We show in Fig. 6 that increasing the training set size increases the test accuracy. The curve levels off around 20,000 trajectory snippets, which corresponds to about 2 weeks of data collection.

### D. Results

With these optimized hyperparameters and training set size, we then trained on 2 weeks of data (22,481 trajectory snippets). The test accuracy was 86.3%. Note that this is higher than the accuracy from hyperparameter optimization because there was more training data.

We show the various combinations of true/predicted labels in Fig. 7, with numerical listings in Table III. On the left (Fig. 7a), we show the trajectory snippets for which our classifier predicted a label of 0. Our accuracy on trajectories that don't cross in front of the vehicle are pretty high. It is interesting to note the rectangular gap in the center; this demonstrates that our classifier learned that trajectories that enter that region should never be classified as 1. There are some red trajectories around the edge of the rectangle which are particularly challenging.

On the right (Fig. 7b), the trajectories our classifier labeled as 1 are relatively somewhat less accurate. Recall that the trajectories are split into snippets, so for long trajectories that are split into many snippets, this classifier seems to perform much worse on the snippets that are far away from the vehicle. It is expected that the performance would be worse further away from the vehicle. Some of the long trajectories are still classified correctly, indicating the classifier is learning some notion of direction, since we are only feeding in pedestrian positions over time.

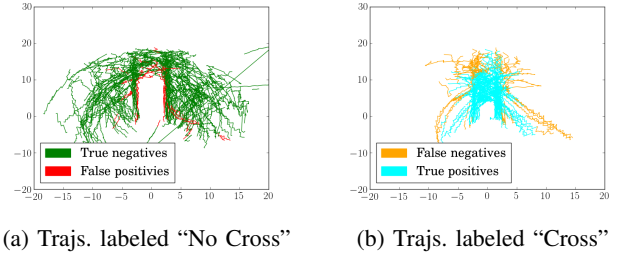


Fig. 7: Predicted labels on test set with SVM classifier. On the left, trajectory snippets that were predicted label 0 (green is correct, red is incorrect). Notice the large rectangular gap in the center, corresponding to learned “cross zone”. On the right, trajectory snippets that were predicted label 1 (cyan correct, orange incorrect). Across the whole test set, 84% accuracy was achieved.

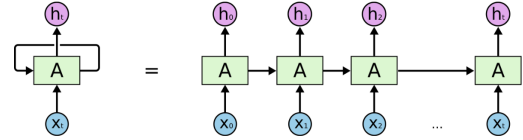


Fig. 8: Illustration of a RNN in its enrolled (left) and unrolled (right) form. Each sequential input  $x_t$  is fed in at timestep  $t$ , transformed by the activation cell  $A$  and output and fed into the next cell as hidden state  $h_t$ . (colah)

### E. Kernel Choice

According to [5], time series data can be classified with a SVM with many different types of kernels, but the most broadly applicable one is Gaussian RBF. Therefore, we used a Gaussian RBF kernel with  $\gamma$  set automatically by SKLearn’s implementation. This kernel allows non-linear combinations of feature elements, which could be useful for this task. Ideally, we would use some kernel that was designed specifically for our time-series trajectory data, but we didn’t focus much on this aspect of the problem. Instead, we considered a different learning method (RNN) to try to better capture the time dependence of our data.

## IV. RECURRENT NEURAL NETWORK: BINARY CLASSIFICATION

We first briefly describe RNNs and LSTMs, as these were not covered in homework assignments. Then, we analyze the performance of an LSTM for the same binary classification as before, and compare with the SVM implementation.

### A. Introduction

Recurrent Neural Networks (RNNs) have been shown to extract sequential information and generate highly complex sequences as documents, translations, music and more. In comparison to n-gram models, which have been used in language model for speech recognition, a RNN makes a prediction by a high-dimensional interpolation between training samples. N-gram models predict by creating a distribution, based on the number of exact matches between the recent history and the training set (graves).

In theory RNNs can be trained by backpropagating the error along the chain of cells. However, every step involves



| Dataset | $l = 2$       |           |           |        |        |        |        | $l = 10$  |           |           |        |        |        |        |
|---------|---------------|-----------|-----------|--------|--------|--------|--------|-----------|-----------|-----------|--------|--------|--------|--------|
|         | $C = 10^{-3}$ | $10^{-2}$ | $10^{-1}$ | $10^0$ | $10^1$ | $10^2$ | $10^3$ | $10^{-3}$ | $10^{-2}$ | $10^{-1}$ | $10^0$ | $10^1$ | $10^2$ | $10^3$ |
| Train   | 70.8          | 83.2      | 84.8      | 85.9   | 87.1   | 89.1   | 91.9   | 63.8      | 76.1      | 84.6      | 86.8   | 92.6   | 97.2   | 99.6   |
| Val     | 63.1          | 77.4      | 79.1      | 78.9   | 78.0   | 77.8   | 77.6   | 60.3      | 67.9      | 78.4      | 79.4   | 79.3   | 77.7   | 76.1   |
| Dataset | $l = 25$      |           |           |        |        |        |        | $l = 50$  |           |           |        |        |        |        |
|         | $C = 10^{-3}$ | $10^{-2}$ | $10^{-1}$ | $10^0$ | $10^1$ | $10^2$ | $10^3$ | $10^{-3}$ | $10^{-2}$ | $10^{-1}$ | $10^0$ | $10^1$ | $10^2$ | $10^3$ |
| Train   | 62.9          | 64.9      | 82.4      | 88.7   | 96.8   | 99.9   | 100    | 60.4      | 60.4      | 77.6      | 92.2   | 99.3   | 100    | 100    |
| Val     | 59.2          | 59.3      | 75.0      | 79.7   | 79.8   | 78.8   | 78.8   | 52.3      | 52.3      | 64.8      | 75.0   | 74.8   | 74.5   | 74.5   |

TABLE II: Accuracy of SVM for various values of hyperparameters  $C$ ,  $l$ .

| Classification  | SVM    |         | LSTM   |         |
|-----------------|--------|---------|--------|---------|
|                 | Number | Percent | Number | Percent |
| False Positives | 100    | 4.5     | 349    | 6.0     |
| False Negatives | 199    | 9.1     | 791    | 13.5    |
| True Positives  | 822    | 37.4    | 1840   | 31.6    |
| True Negatives  | 1077   | 49.0    | 2850   | 48.9    |
| Total           | 2198   | 100.0   | 5830   | 100.0   |

TABLE III: Classification matrix

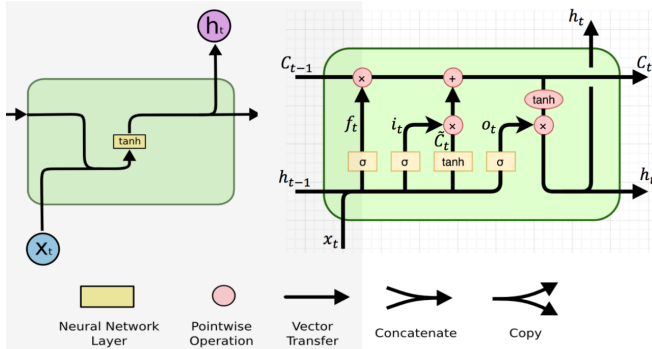


Fig. 9: Activation cell of a traditional RNN (top) and a LSTM (bottom). LSTM propagates the cell  $c_t$  and hidden  $h_t$  state. With ignoring the forget gate  $f_t$ ,  $c_t$  is only updated by sum operations. The gradient along a sum-operation splits up equally and thereby allows to propagate until the beginning of the sequence without vanishing. ResNets have introduced a similar change in the CNN architecture (resnet paper). (changhau)

a multiplication with the weight matrix  $W$ , which, in many cases, results in either an exploding or vanishing gradient (see class exercise). The exploding/vanishing gradient problem is, in practice, addressed by gradient clipping (cs232 lecture). **M. E. are these 2 diff methods to address vanishing gradient problem?** The *vanishing gradient problem* is leveraged by a specific architecture of RNNs, called *Long Short-term Memory* (LSTM) networks. LSTMs split up the RNN's hidden state into a hidden and a cell state. The cell state, similar to in ResNets, is updated by a sum-operation, rather than a whole transformation **M. E. unclear** (SEE FIGURE ... for the comparison of RNN to LSTM cell). The gradient along a sum-operation splits up equally and thereby allows to propagate until the beginning of the sequence without vanishing. **M. E. unclear**

The LSTM is computed according to the following com-

posite function **M. E. add citation** (graves):

$$\begin{aligned}
 i_t &= \sigma(W_{xi}x_t + W_{hi}h_{t-1} + W_{ci}c_{t-1} + b_i) \\
 f_t &= \sigma(W_{xf}x_t + W_{hf}h_{t-1} + W_{cf}c_{t-1} + b_f) \\
 c_t &= f_t c_{t-1} + i_t \tanh(W_{xc}x_t + W_{hc}h_{t-1} + b_c) \quad (1) \\
 o_t &= \sigma(W_{xo}x_t + W_{ho}h_{t-1} + W_{co}c_{t-1} + b_o) \\
 h_t &= o_t \tanh(c_t)
 \end{aligned}$$

where  $\sigma$  is the sigmoid function,  $i_t$ ,  $f_t$ ,  $o_t$  and  $c_t$  are the input gate, forget gate, output gate and cell activation vectors. All weight matrices have the same meaning, for example  $W_{hf}$  is the hidden-forget weight matrix. **M. E. same meaning?** For clarity, bias terms are omitted **M. E. from what?** Figuratively speaking, the input gate regulates how much information is taken from the new input  $x_t$ . The forget gate can erase the cell memory and thereby controls the duration of time dependency during sequence prediction. The cell state is the part of memory that propagates between hidden nodes. The output gate regulates how much information from the hidden cell state is propagated into the output hidden state.

### B. LSTMs for binary classification

We used LSTM networks for the same binary classification task from Section III. LSTMs are able to extract the sequential information more naturally than SVM, so we expected to see better classification accuracy in the train and test datasets. We used Python and the *Tensorflow* library to implement the LSTMs.

Again, the full trajectories have been precompiled into snippets of static sequence length  $T$ . At each time step, the input vector is the relative pedestrian position at time  $t$ :  $x_t \in \mathbb{R}^{1 \times 2}$ . For binary classification, we use a many-to-one architecture. The output is calculated at the output layer by using a logistic sigmoid for binary classification:

$$y_t = \sigma(W_{hout}h_t + b_{out}) \quad (2)$$

where  $y_t \in [0, 1]$ ,  $W_{hout} \in \mathbb{R}^{n_{hidden} \times 1}$ , and  $n_{hidden}$  is the number of hidden units. The weight matrices and biases are initialized with random noise  $\sim \mathcal{N}(0, 1)$ . We use the least mean squared error (LMSE) loss function. The network is optimized by a stochastic gradient descent (SGD) method with the goal to minimize the loss over the weight matrices and their biases.

### C. Hyperparameters

Again, there are many hyperparameters to optimize, including the number of hidden units, batch size, learning rate, and

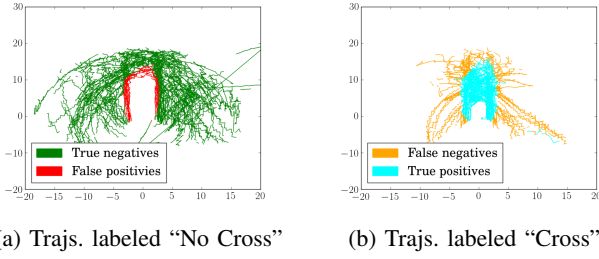


Fig. 10: Predicted labels on test set with LSTM classifier. On the left, trajectory snippets that were predicted label 0 (green is correct, red is incorrect). On the right, trajectory snippets that were predicted label 1 (cyan correct, orange incorrect). Across the whole test set, 80% accuracy was achieved. Compare with Fig. 7

number of training epochs. It is very time intensive to search over all hyperparameters. We briefly summarize the hyperparameters' effects on performance, using validation accuracy as the performance metric. The output of our full grid search is in our posted code (file: rnn\_classifier\_hyperparameters.txt).

The best hyperparameters were batch size of 5,  $n_{hidden} = 256$ ,  $T = 10$ , and 3 training epochs, and we used a learning rate of 0.001.

Performance generally levels off after 3-5 training epochs. For large  $T$ , more hidden units are required to handle the higher dimension of the input data. Specifically, when  $T > 10$ ,  $n_{hidden} = 8$  got  $< 50\%$  accuracy, but performance improved with  $n_{hidden} = 64$  (we ranged  $T$  from 2-50, and  $n_{hidden}$  from 8-256). Small batch size tended to improve the performance, but it was not a clear trend (we ranged batch size from 1-10).

We also investigate the effect of training set size on performance in Fig. 6. The blue line corresponds to the LSTM classifier, which is not greatly affected by training set size (close to 80% throughout). The LSTM classifier is not as sensitive as SVM to training set size.

#### D. Results

After optimizing hyperparameters and confirming we have a sufficient amount of training data, we trained the LSTM binary classifier. The overall test accuracy was 80.4%.

Fig. 7 & Fig. 10 look pretty similar. Both classifiers learned about the "cross zone", perform relatively well on data that is predicted to be class 0, and struggle with false negatives far from the vehicle. The fact that both classifiers indicates that type of data is especially challenging to classify correctly.

### V. RECURRENT NEURAL NETWORK: PREDICTION

#### A. Introduction

Recurrent Neural Networks (RNNs) have been shown to extract sequential information and generate highly complex sequences as documents, translations, music and more. In comparison to n-gram models, which have been used in language model for speech recognition, a RNN makes a prediction by a high-dimensional interpolation between training samples. N-gram models predict by creating a distribution, based on the number of exact matches between the recent history and the training set (graves).

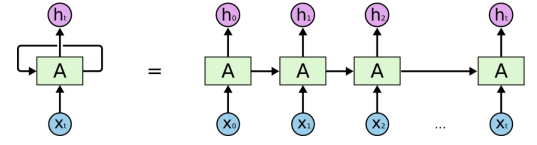


Fig. 11: Illustration of a RNN in its enrolled (left) and unrolled (right) form. Each sequential input  $x_t$  is fed in at timestep  $t$ , transformed by the activation cell  $A$  and output and fed into the next cell as hidden state  $h_t$ . (colah)

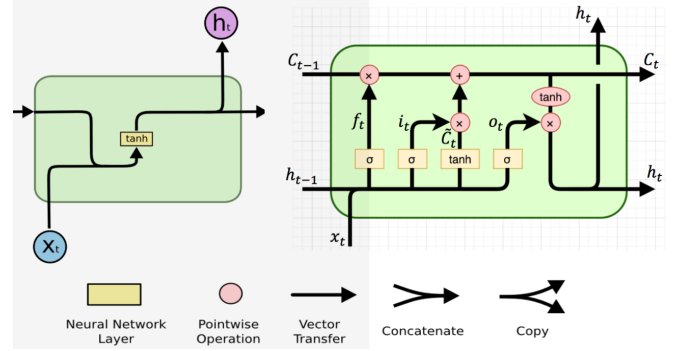


Fig. 12: Activation cell of a traditional RNN (top) and a LSTM (bottom). LSTM propagates the cell  $c_t$  and hidden  $h_t$  state. With ignoring the forget gate  $f_t$ ,  $c_t$  is only updated by sum operations. The gradient along a sum-operation splits up equally and thereby allows to propagate until the beginning of the sequence without vanishing. ResNets have introduced a similar change in the CNN architecture (resnet paper). (changhau)

In theory RNNs can be trained by backpropagating the error along the chain of cells. However, every step involves a multiplication with the weight matrix  $W$ , which, in many cases, results in either an exploding or vanishing gradient (see class exercise). The exploding gradient problem is, in practice, leveraged by gradient clipping (cs232 lecture). The *vanishing gradient problem* is leveraged by a specific architecture of RNNs, called *Long Short-term Memory* (LSTM) networks. They are splitting up the RNNs hidden state into a hidden and a cell state, whereas the cell state, like ResNets, is updated by a sum-operation, rather than a whole transformation (SEE FIGURE ... for the comparison of RNN to LSTM cell). The gradient along a sum-operation splits up equally and thereby allows to propagate until the beginning of the sequence without vanishing.

The LSTM is computed according to the following composite function (graves):

$$\begin{aligned} i_t &= \sigma(W_{xi}x_t + W_{hi}h_{t-1} + W_{ci}c_{t-1} + b_i) \\ f_t &= \sigma(W_{xf}x_t + W_{hf}h_{t-1} + W_{cf}c_{t-1} + b_f) \\ c_t &= f_t c_{t-1} + i_t \tanh(W_{xc}x_t + W_{hc}h_{t-1} + b_c) \\ o_t &= \sigma(W_{xo}x_t + W_{ho}h_{t-1} + W_{co}c_{t-1} + b_o) \\ h_t &= o_t \tanh(c_t) \end{aligned} \quad (3)$$

where  $\sigma$  is the sigmoid function,  $i_t$ ,  $f_t$ ,  $o_t$  and  $c_t$  are the input gate, forget gate, output gate and cell activation vectors. All weight matrices have the same meaning, for example  $W_{hf}$  is the hidden-forget weight matrix. For clarity, bias terms

are omitted. Figuratively speaking, the input gate regulates how much information is taken from the new input  $x_t$ . The forget gate can erase the cell memory and thereby shorten or lengthen the time dependency of a sequence prediction. The cell state is the propagated memory. The output gate regulates how much information from the hidden cell state is propagated into the output hidden state.

### B. LSTMs for binary classification

We have used LSTM networks for the same binary classification task, as for SVMs. LSTMs are able to extract the sequential information and should thereby provide better classification accuracy in the train and test dataset. All calculations have been done in python and the network has been set up with the *tensorflow* library.

The full trajectories have been precompiled into snippets of static sequence length  $T$ . At each time step, the input vector is the relative pedestrian position at time  $t$ :  $x_t \in \mathbb{R}^{1 \times 2}$ . For binary classification, we use a many-to-one architecture. The output is calculated at the output layer by using a logistic sigmoid for binary classification:

$$y_t = \sigma(W_{\text{hout}}h_t + b_{\text{out}}) \quad (4)$$

where  $y_t \in [0, 1]$  and  $W_{\text{hout}} \in \mathbb{R}^{(n_{\text{hidden}} \times 1)}$ , where  $n_{\text{hidden}}$  is the number of hidden units. The weight matrices and biases are initialized with random noise  $N(0, 1)$ . The loss is computed with least mean squared error (LMSE). The system is optimized by a stochastic gradient descent (SGD) method with the goal to minimize the loss over the weight matrices and their biases.

1) *Hyperparams in bin class*: - Optimize number of hidden units - batchsize - learning rate - maximum epochs  
 - challenge: predict real-valued sequence - low dimensionality and ease of visualization - no sophisticated preprocessing or feature-extraction techniques (graves p.18) - reduce variation in data (normalize character size, slant, skew,) - Compare our dataset to handwritten dataset size (graves p.18) - handwriting has 25 timesteps per character and 700 timesteps per line - 5000 training, two val of 1500 lines, test 4000 lines (each line 700 timesteps)

## VI. RECURRENT NEURAL NETWORK

### A. Introduction

### B. Network architecture

- explain  $x_t$  - feeding relative x and y would not respect car position and its influence on pedestrian behavior - explain  $y_t$  - copy picture of LSTM from GRAVES

### C. GRUs

From: <http://www.jackdermody.net/brightwire/article/Sequence-to-sequence-with-LSTM>

Long Short Term Memory (LSTM) networks are a recurrent neural network that can be used with STS neural networks. They are similar to Gated Recurrent Units (GRU) but have an extra memory state buffer and an extra gate which gives them more parameters and hence a longer training time. While

performance with GRU is usually comparable, there are some tasks that each architecture outperforms the other on, so comparing each for a given learning task is usually a good idea.

### D. Training

- random batch selection - Optimizer - Gradient Descent - use momentum?

1) *Hyperparameters*: - Dropout? - `cell = tf.contrib.rnn.DropoutWrapper(cell, output_keep_prob = args.keep_prob)`

2) *Regularization*: - Random weight initialization - See graves (p.7), weight noise, adaptive weight noise - use validation set for early stopping - Gradient clipping? - could prove vital for numerical stability

### E. Results

- print total loss - print avg LSE per datapoint

### F. Resources

colah <http://colah.github.io/posts/2015-08-Understanding-LSTMs/> changhau <https://isaacchanghau.github.io/2017/07/22/LSTM-and-GRU-Formula-Summary/>

### DIVISION OF LABOR & LINK TO CODE

Michael mostly worked on the dataset processing and SVM/RNN classifier optimization, and Björn did the RNN prediction/classifier implementations and the rest of the SVM work. We have been a 2-person team since Milestone 2. This project is not used for any other classes. Our code can be found at: <https://github.com/mfe7/6.867>.

### REFERENCES

- [1] J. Miller, A. Hasfura, S.-Y. Liu, and J. P. How, "Dynamic arrival rate estimation for campus mobility on demand network graphs," in *IEEE/RSJ International Conference on Intelligent Robots and Systems (IROS)*, 2016.
- [2] J. Miller and J. P. How, "Predictive positioning and quality of service ridesharing for campus mobility on demand systems," in *IEEE International Conference on Robotics and Automation (ICRA)*, 2017.
- [3] Anonymous, "CASNSC: A context-based approach for accurate pedestrian motion prediction at intersections," <https://openreview.net/pdf?id=rJ26HSLRb>, 2017, [Online; accessed 12-Dec-2017].
- [4] F. Pedregosa, G. Varoquaux, A. Gramfort, V. Michel, B. Thirion, O. Grisel, M. Blondel, P. Prettenhofer, R. Weiss, V. Dubourg, J. Vanderplas, A. Passos, D. Cournapeau, M. Brucher, M. Perrot, and E. Duchesnay, "Scikit-learn: Machine learning in Python," *Journal of Machine Learning Research*, vol. 12, pp. 2825–2830, 2011.
- [5] S. Rüping, "Svm kernels for time series analysis," 2001.